Mg^{2+}-paracrystal formation of tropomyosin as a condensation phenomenon

Effects of pH, salt, temperature, and troponin binding

Yoshiharu Ishii and Sherwin S. Lehrer

Department of Muscle Research, Boston Biomedical Research Institute, Boston, Massachusetts 02114; and the Department of Neurology, Harvard Medical School, Boston, Massachusetts 02115

ABSTRACT Tropomyosin (Tm) paracrystal formation induced by Mg^{2+} was studied by monitoring increases in light scattering. Paracrystals formed above a critical Tm concentration with lag phases in the time courses at pH 7.5 and 6.0, indicating that condensation polymerization processes are involved. The kinetic data at pH 7.5 reasonably fit a model in which nucleation and elongation are taken into account. The rate and extent of light scattering increased at low [Mg^{2+}] and decreased at high [Mg^{2+}] with a maximum at [Mg^{2+}] = 15 mM, indicating different effects of Mg^{2+} in the two [Mg^{2+}] ranges. The paracrystals were destabilized by increasing the salt concentration and decreasing the temperature. Mg^{2+} produces paracrystals at pH 6.0 and pH 7.5 by different kinetic mechanisms. Different Tm intermolecular interactions at the two pH values were indicated by studies of the excimer fluorescence of pyrene-labeled Tm and by effects of salt and temperature on the kinetics. At pH 6.0 Tm more readily formed paracrystals with decreased electrostatic effects. Effects of troponin on Mg^{2+}-paracrystal formation of Tm at the two pH values correlated with the known differences in paracrystal structure when troponin is bound to Tm.

INTRODUCTION

Tropomyosin (Tm), a component of vertebrate skeletal and cardiac muscle, plays a role in the Ca^{2+} regulation of muscle contraction in conjunction with troponin (Ebashi and Endo, 1968; Smillie, 1979; Leavis and Gergely, 1984). Tm aggregates in solution both by side-to-side and end-to-end molecular interaction (Ooi et al., 1962). It also forms a variety of crystals and paracrystals at low pH and by binding of divalent cations (Cohen and Longley, 1966; Caspar et al., 1969), resulting in different molecular arrangements. Paracrystals formed in the presence of Mg^{2+} or Ca^{2+}, show a clear longitudinal repeat of 400 A at pH 7 and above, while at low pH (<6) the paracrystals show oblique striations spaced ~50 and 70 A, indicating different intermolecular Tm interactions at low and high pH (Cohen and Longley, 1966; Casper et al., 1969; Nonomura, 1968; Longley, 1977; Katayama and Nonomura, 1979).

Studies on the formation of assembly of F-actin, microtubules, bacterial flagella, intermediate filaments, myosin thick filaments, and tobacco mosaic virus have shown a lag phase in the time course and a minimum concentration (critical concentration) necessary for assembly (Oosawa and Asakura, 1975). These phenomena have been explained in terms of a condensation polymerization process with the involvement of nucleation and elongation steps.

Address correspondence to Department of Muscle Research, Boston Biomedical Research Institute, Boston, MA 02114.

Here, Tm paracrystal formation induced by Mg^{2+} was also shown to be a helical polymerization process involving one-dimensional growth (Oosawa 1962). Within the general theory different mechanisms for formation of paracrystals are proposed at pH 6 and 7.5 that correspond to the different paracrystal forms observed by electron microscopy. A good correlation between Tm paracrystal formation and paracrystal structure was also obtained for the complex with troponin.

MATERIALS AND METHODS

Tm and troponin were prepared from rabbit skeletal muscle by standard procedure (Lehrer and Morris, 1982) and pyrene-maleimide labeled Tm was prepared as previously described (Graceffa and Lehrer, 1980).

Paracrystal formation was measured by 90° light scattering at 350 nm in a Fluorolog 2/2/2 fluorometer (Spex Industries, Inc., Edison, NJ) or by absorbance (turbidity) at 350 nm in a λ-3 spectrophotometer (Perkin-Elmer Corp. Instruments Div., Norwalk, CT). Both methods gave the same result when the absorbance was <0.15. For solutions of absorbance >0.15, turbidity measurements were used because 90° light scattering was not proportional to turbidity. The absorbance and light scattering were determined within ±5%. The monomer and excimer fluorescence components of pyrene-Tm were excited at 340 nm and measured at 385 and 485 nm, respectively, in the fluorometer (Spex Industries, Inc.). The centrifugation experiments were carried out in a airfuge (Beckman Instruments Inc., Palo Alto, CA) and the protein concentration in the supernatant was determined by BCA protein assay (Pierce Chemical Co., Rockford, IL). The data were reproducible within ±8%. Calculations and curve fitting were done with programs developed using the Datamate (Spex Industries, Inc.) computer.

0006-3495/89/07/107/08 $2.00

THEORETICAL ANALYSIS

Paracrystal formation of Tm caused by the binding of Mg^{2+} is considered to be a condensation polymerization process consisting of two steps; the formation of a nucleus made up of i monomer molecules (Eq. 1) and an elongation step of a j-mer to a $(j + 1)$-mer by the attachment of a free monomer molecule (Eq. 2) (Oosawa and Asakura 1975):

$$iM \underset{k_{n-}}{\overset{k_{n+}}{\rightleftharpoons}} M_i \quad \text{(nucleation)} \tag{1}$$

$$M_j + M \underset{k_{e-}}{\overset{k_{e+}}{\rightleftharpoons}} M_{j+1} \quad \text{(elongation).} \tag{2}$$

The rate equations are

$$dm/dt = k_{n+}c_1^i - k_{n-}c_i \quad \text{(nucleation)} \tag{3}$$

$$dc_a/dt = -dc_1/dt = (k_{e+}c_1 - k_{e-})m \quad \text{(elongation),} \tag{4}$$

where m is the number concentration of paracrystals, c_1, c_i, and c_a the concentration of dispersed Tm, i-mers, and monomers participating in the paracrystals, respectively. An analytical solution for c_1 and c_a can only be obtained if the reverse processes are neglected. Alternatively, solutions can generally be obtained by numerical integration with a computer. Fragmentation,

$$M_{i+j} \xrightarrow{k_{fr}} M_i + M_j \tag{5}$$

can be incorporated in Eq. 3 by including a term for the number concentration of paracrystals produced by fragmentation, $k_{fr}(c_o - c_1)$ (Oosawa and Asakura, 1975; Wegner and Savko, 1982). The critical concentration, c_c, is given by $dc_a/dt = 0$ in Eq. 4, that is, $c_c = k_{e-}/k_{e+}$.

The monomer concentrations dispersed and participating in the polymers are approximately determined by total and critical concentrations, c_o and c_c, respectively.

For $c_o < c_c$;

$$c_1 = c_o, c_a = 0$$

for $c_o > c_c$;

$$c_1 = c_c, c_a = c_o - c_c$$

when c_o is total concentration.

Experimentally c_a can be measured from the light scattering increase and c_1 can be measured from the Tm concentration in the supernatant after centrifugation. For the fitting of the kinetics of paracrystal formation there are six parameters to be considered, four rate constants, the size of nucleus, i, and α, a constant to relate the Tm concentration to the light scattering increment. The rate of shortening is related to the rate of elongation using the critical concentration ($k_{e-} = c_c k_{e+}$). Analogously, for nucleation process, the kinetic equation can be approximated by $dm/dt = (k'_{n+}c_1 - k'_{n-})c_1^{i-1}$ and $k'_{n-} = c_c k'_{n+}$, when $k'_{n\pm}$ are proportional to $k_{n\pm}$ (Wegner and Engel, 1975). The product of the two rate constants $k = k'_{n+}k_{e+}$ mainly determines the kinetic profile of c_a as shown in the analytical solutions (Oosawa and Asakura, 1975). Thus, the parameters to be determined are reduced to k, i, c_c, and α. First, c_c and α were estimated from the [Tm] dependence of light scattering intensity; c_c was determined by extrapolating the linear curves of light scattering vs. Tm concentration to zero light scattering intensity and α was determined from the slope. Then, the best parameters for k and i were searched to minimize the deviation between a set of calculated and experimental kinetic data at different Tm concentrations.

RESULTS

The addition of 10–30 mM Mg^{2+} to micromolar concentrations of Tm in solution causes an increase in turbidity as measured by 90° light scattering or absorbance (Figs. 1 and 5). This is the result of the formation of typical needle-like paracrystals observed with phase contrast and fluorescence microscopy on labeled Tm (Lehrer and Ishii, 1988). Different kinetic curves are obtained at pH 7.5 and 6.0, corresponding to the different types of paracrystals of Tm reported previously (Cohen and Longley, 1966; Caspar et al., 1969; Nonomura, 1968; Longley, 1977; Katayama and Nonomura, 1979). At pH 7.0 the kinetic curves were complicated suggesting that both mechanisms appeared to contribute to form a mixture of the two types of paracrystals.

1. High pH paracrystal (pH 7.5)

At pH 7.5 the light scattering increased after a short lag and reached a plateau (Fig. 1). Because Tm is known to polymerize in an end-to-end fashion in the absence of salt, the presence of polymers in the initial state of Tm might affect the kinetic profile. Preincubation with 1–3 mM Mg^{2+} for ~10 min, which is known to depolymerize Tm to a large degree, did not change the kinetic profile. Thus the lag phase was not due to depolymerization or dissociation of any initial aggregates, but due to time effects involved in the nucleation of paracrystals.

The final light scattering intensity increased linearly with the Tm concentration above a critical concentration (Fig. 2). Centrifugation studies also indicated that a critical concentration of Tm was required to form paracrystals, i.e., the Tm concentration in the supernatant increased to a constant value (the critical concentration)

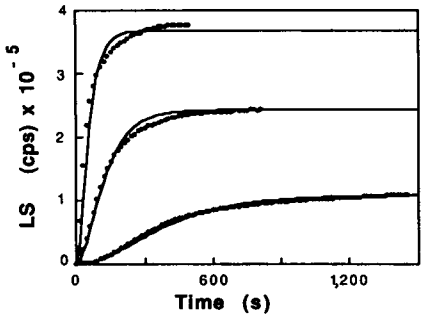

FIGURE 1 Kinetics of Mg^{2+}-paracrystal formation of Tm at pH = 7.5 at different Tm concentrations. Paracrystal formation was monitored by light scattering after 20 mM $MgCl_2$ was added at time = 0. 10 mM Hepes, pH = 7.5, 25°C, [Tm] = 1.54 μM (*top*), 1.23 μM (*middle*), and 0.89 μM (*bottom*), respectively. Theoretical curves (*solid line*) were calculated with the scheme presented in Theoretical Analysis using i = 5, $k = k'_{n+}k_{e+} = 7.0 \times 10^{20}\ s^{-2}M^{-5}$, c_c = 0.62 μM and light scattering increment = 4×10^5 cps/μM Tm.

as the total concentration increased. Thus light scattering is proportional to the Tm concentration in the paracrystals and this parameter was therefore used for quantitative kinetic and static studies of paracrystal formation. The kinetic data were fit to the scheme as outlined in the Theoretical Analysis and as can be seen gave reasonable agreement (Fig. 1). The critical concentration was estimated to be (0.62 ± 0.02) μM by extrapolating the light scattering data to the abscissa. The size of nucleus, i, was estimated to be 5 ± 1 and the overall rate constant, $k = k'_{n+}k_{e+}$, (7.0 ± 0.5) × $10^{20}\ s^{-2}M^{-5}$ at 20 mM Mg^{2+}, 25°C. The kinetic profile of the paracrystal formation was thus explained essentially by the condensation polymerization process which consists of nucleation and elongation steps.

Addition of NaCl slowed the paracrystal formation and reduced a magnitude by increasing the critical concentration. The overall rate constant k decreased from (7.0 ± 0.5) × 10^{20} to (1.0 ± 0.1) × $10^{20}\ s^{-2}M^{-5}$ in the presence of 3 mM NaCl and the critical concentration increased from (0.62 ± 0.02) to (1.02 ± 0.02) μM (data not shown). When the Mg^{2+} concentration was changed at a constant Tm concentration (1.23 μM), the final light scattering change and apparent rate (reciprocal of half-time) showed two different effects of Mg^{2+} below and above an optimum Mg^{2+} concentration of ~15 mM (Fig. 3). To explore how Mg^{2+} induces paracrystal formation at low Mg^{2+} concentration and inhibits paracrystal formation at high Mg^{2+} concentration, the Tm concentration dependence was studied below and above the optimum Mg^{2+} concentration.

At high Mg^{2+} concentrations (>15 mM) the equilibrium experiments with both light scattering and centrifugation showed that the critical concentration increased with Mg^{2+} (Fig. 4; $[Tm]_c$ = (0.35 ± 0.01, 0.62, and 1.00 ± 0.02 μM at 15, 20, and 25 mM Mg^{2+}, respectively. The data for [Mg^{2+}] = 25 mM not shown in Fig. 4) and the kinetic experiments showed that the overall rate was slowed (k = (10.5 ± 0.5), (7.0 ± 0.2), and (1.5 ± 0.1) × $10^{20}\ s^{-2}M^{-5}$ at 15, 20, and 25 mM Mg^{2+}, respectively). At low Mg^{2+} (<15 mM) no light scattering was observed below [Tm] = 0.5 μM and then the light scattering increased gradually with Tm concentration consistently with centrifuge experiments which showed that the dispersed Tm concentration was the same as total Tm concentration below [Tm] = 0.5 μM and then gradually reached a plateau. The dashed lines in Fig. 4 were drawn in using the assumption that the light scattering increases with the same slope as in high Mg^{2+} concentration above the critical concentration and dispersed Tm concentration

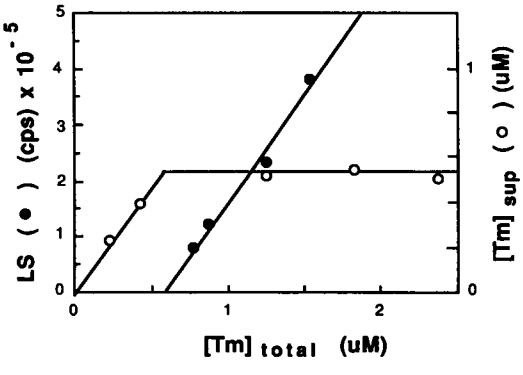

FIGURE 2 Tm concentration dependence of the extent of paracrystal formation at pH 7.5. Final light scattering change (●) taken from Fig. 1 and [Tm] in supernatant after pelleting paracrystals, $[Tm]_{sup}$, under the same experimental conditions as Fig. 1 (○).

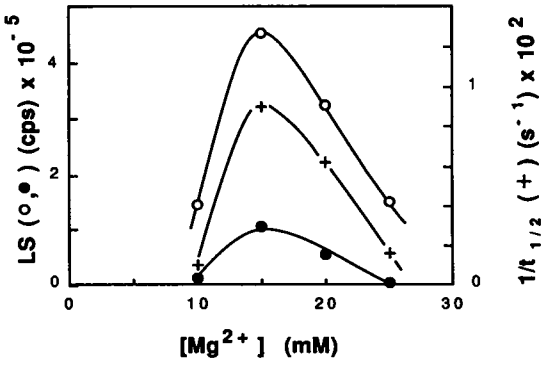

FIGURE 3 Mg^{2+} concentration dependence of paracrystal formation at pH 7.5, 25°C. Final light scattering change, (○), and reciprocal of half time, $1/t_{1/2}$ (+). Light scattering change at 5°C (●) was measured 10 d after $MgCl_2$ addition. [Tm] = 1.23 μM, 10 mM Hepes.

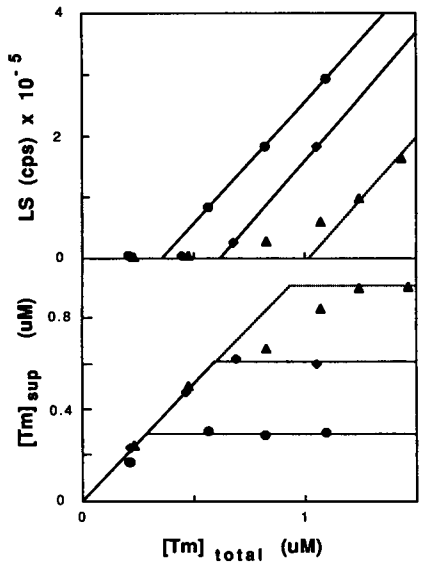

FIGURE 4 Tm concentration dependence of the extent of paracrystal formation at pH 7.5 for various Mg^{2+} concentrations. (*Upper*) light scattering change 2 h after addition of $MgCl_2$. This represents the Tm concentration in the paracrystal. Lower: $[Tm]_{sup}$, represents Tm concentrations not in paracrystals. $[Mg^{2+}]$ is 10 (▲), 15 (●), and 20 mM (◆). Buffer is 10 mM Hepes (pH 7.5), 25°C. Dashed lines represent extrapolated values.

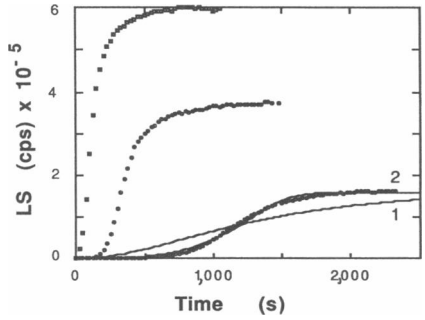

FIGURE 5 Kinetics of Mg^{2+}-paracrystal formation at pH = 6.0. Light scattering change was monitored after addition of 15 mM $MgCl_2$ at time = 0.20 mM NaCl, 10 mM Mes (pH 6.0). Tm concentrations are 1.76, 1.32, and 0.88 μM from the top. Two theoretical curves were calculated (1) without fragmentation using $i = 5$, $k = 1.5 \times 10^{20} s^{-2}M^{-5}$, (2) with fragmentation using $i = 5$, $k = 0.3 \times 10^{20} s^{-2}M^{-5}$, $k_{fr} = 2.2 \times 10^{-7} s^{-1}$.

reaches critical concentration. The critical concentration obtained was 0.9 ~ 1.0 μM.

Temperature was another parameter to determine the ability of Tm to form paracrystals. At 15°C the apparent rate was slowed from $(1.4 \pm 0.1) \times 10^{-2}$ s^{-1} at 25°C to 3.3×10^{-3} s^{-1} at 15 mM $MgCl_2$. At equilibrium the light scattering more gradually increased with Tm concentration reaching to an asymptote with the same slope as at 25°C at high Tm concentrations and the critical concentration was greater (>1.2 μM). The Mg^{2+} concentration dependence was not changed (Fig. 3).

2. Low pH paracrystal (pH = 6.0)

At pH = 6.0 the kinetics after addition of 15 mM $MgCl_2$ showed that the lag phase was more prominent than at pH 7.5 (Fig. 5). In the absence of NaCl the final light scattering change vs. total Tm concentration gave a straight line through the origin (Fig. 6); i.e., the critical concentration was zero indicating that all the Tm molecules were in the paracrystals. This was confirmed by centrifuge experiments, which showed that there was little Tm in the supernatant at all Tm concentration studied.

The effects of NaCl at pH = 6.0 on paracrystal formation were similar to that at pH 7.5, but a greater NaCl concentration was required to produce the same change. When 20 mM NaCl was present in addition to 15 mM Mg^{2+}, the critical concentration became nonzero (0.47 ± 0.03) μM showing that the dissociation process cannot be ignored in the presence of NaCl. This Na^+ effect did not appear to be due to competitive binding with Mg^{2+} because at low Mg^{2+} concentration (2 mM) 20 mM NaCl increased the critical concentration to a similar extent as at 15 mM $MgCl_2$. Consistently with effects on the critical concentration, NaCl influenced the dissociation rate. This was measured by diluting a suspension of Tm paracrystals into solutions of various NaCl concentration in the absence of Mg^{2+}. In the absence of NaCl the light scattering decreased slowly with the rate of 6.3×10^{-4} s^{-1} and dissociation rate increased to 0.01 and 0.2 s^{-1} by addition of 5 and 10 mM NaCl, respectively.

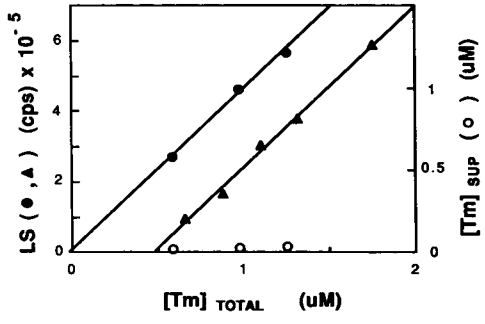

FIGURE 6 Tm concentration dependence of the extent of paracrystal formation at pH 6.0. Light scattering change was measured at 0 (●) and 20 mM NaCl (▲) and $[Tm]_{sup}$ was determined by sedimentation of paracrystals without NaCl (○). $[MgCl_2]$ = 15 mM, 10 mM Mes (pH 6.0).

The Mg^{2+} concentration dependence of paracrystal formation below and above 15 mM were different at pH 6.0 (Fig. 7). Below 15 mM Mg^{2+} Tm formed paracrystals more readily than at pH 7.5; i.e., only ~ 2 mM Mg^{2+} was sufficient in the absence of NaCl. When the Mg^{2+} concentration increased up to 5 ~ 10 mM, the lag time was shortened and the turbidity rise became steeper, but the final change was not altered. Thus at low Mg^{2+} concentrations, the critical concentration was zero. At high Mg^{2+} concentrations (15–35 mM), the turbidity increased more gradually with time resulting in a decrease in the apparent rate ($1/t_{1/2}$) and the final turbidity change increased with Mg^{2+} concentration. Because there was little dispersed Tm left even at low Mg^{2+} concentration, the turbidity increase above 15 mM Mg^{2+} might be due to a different form of aggregates, e.g., a cluster of paracrystals. This high Mg^{2+} form could not readily be produced from the low Mg^{2+} form by a further increase in the Mg^{2+} concentration (see Fig. 7). This indicates that the two forms do not rapidly equilibrate. Above 40 mM Mg^{2+} the aggregation finally disappeared.

The paracrystals were destabilized by a decrease in temperature. Lowering the temperature drastically retarded the onset of the light scattering rise phase without changing the final light scattering intensity at low Mg^{2+} concentration (2.5 mM); e.g., decreasing the temperature from 25°C to 22°C increased the half maximum time from ~4 min. to 25 min. After a long incubation (10 d) at 5°C the turbidity change, which was smaller than at 25°C, had a maximum at 10 mM $MgCl_2$ and the increase in aggregation at high $MgCl_2$ concentration observed at room temperature was completely abolished (Fig. 7).

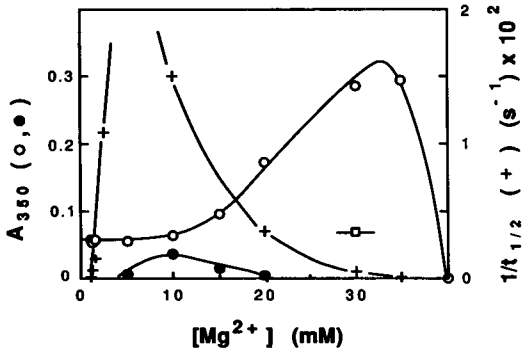

FIGURE 7 Mg^{2+} concentration dependence of paracrystal formation at pH 6.0. Symbols are the same as Fig. 3. (□) Tm was first incubated at [$MgCl_2$] = 5 mM to form low [Mg^{2+}] paracrystals and then additional $MgCl_2$ was added to final concentration of 30 mM. Turbidity stayed constant for at least 24 h after the second addition of $MgCl_2$. The half-time for [Mg^{2+}] ~ 5mM was too fast to measure (the half-time was <5 s.).

3. Two different paracrystal forms at low and high pH evidenced by excimer fluorescence

Pyrene-maleimide labeling of Tm did not affect the Mg^{2+}-induced light scattering change. On increasing Tm concentration the excimer to monomer fluorescence intensity ratio (E/M ratio) increased from the values associated with noninteracting Tm molecules due to intramolecular pyrene-pyrene interaction (Graceffa and Lehrer, 1980). At pH = 7.5 a large increase in the E/M ratio took place. The increase in the E/M ratio as the added Tm concentration increased was proportional to the fraction of Tm in the paracrystal phase estimated from the increase in light scattering (Fig. 8). This indicated that the excimer increase was due to intermolecular rather than intramolecular pyrene-pyrene interaction. In agreement with that concept, in mixtures of labeled and unlabeled Tm the E/M ratio corresponded to the sum of the contribution of the unlabeled Tm and labeled Tm (data not shown). At pH = 6.0 the E/M ratio hardly increased despite a large increase in light scattering (Fig. 8). This indicates that the side-by-side contacts of Tm in the paracrystal are such that the pyrene moieties at Cys positions of neighbor molecules are close enough to interact at pH = 7.5, and too far apart to interact at pH 6.0.

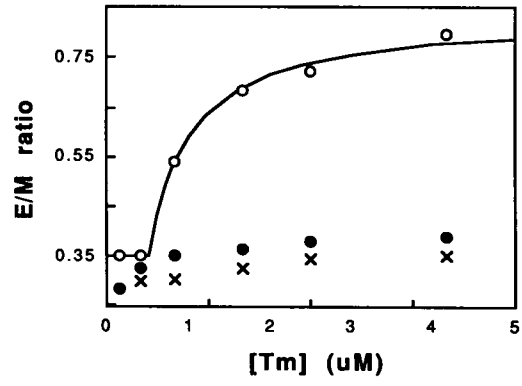

FIGURE 8 Excimer fluorescence increase of pyrene labeled Tm caused by Mg^{2+}-paracrystal formation at pH 7.5 and pH 6.0. Excimer to monomer fluorescence intensity ratio (E/M ratio) of labeled Tm was measured as a function of [Tm] after paracrystal formation was complete. (○) pH 7.5 (20 mM Hepes), 20 mM $MgCl_2$, 25°C. The theoretical curve (*solid line*) is drawn assuming that E/M ratio increase is proportional to the fraction of Tm in paracrystal phase, f_p; $E/M = (E/M)_f f_p + (E/M)_0 (1 - f_p), f_p = 0$ (for $c_o < c_c$) or $(c_o - c_c)/c_o$ (for $c_o > c_c$). C_c for labeled Tm was estimated to be 0.5 μM from light scattering change. Initial E/M, $(E/M)_0$ was 0.35 and final E/M, $(E/M)_f$ was obtained 0.845 for the best fit. (X) E/M ratio in the absence of Mg^{2+} (10 mM NaCl) at pH 7.5 as a control. (●) pH = 6.0 (20 mM Mes), 20 mM $MgCl_2$. Data were taken 16 h after the addition of $MgCl_2$.

4. Paracrystals of tropomyosin-troponin

Addition of troponin to Tm increased the rate of Tm paracrystal formation at both pH 6.0 and 7.5 (data not shown). At pH 7.5, troponin decreased the critical concentration from 0.35 μM to 0.25 μM at 15 mM Mg^{2+}, but the Mg^{2+} concentration dependence did not appear to change (Fig. 9). At both lower and higher Mg^{2+} concentration (5 and 30 mM) the critical concentration increased. Thus Mg^{2+} effects in the presence of troponin were the same as in its absence. At pH 6.0, the Mg^{2+} dependence was rather similar to that at pH 7.5 (Fig. 9). However, the critical concentration was <0.1 μM and the slope of absorbance vs. Tm concentration depended on Mg^{2+} concentration different from the dependence in the absence of troponin between 5 and 25 mM. Thus Tm seems to form paracrystals in the presence of troponin in a different way from Tm alone at pH 6.0. Little or no Ca^{2+} sensitivity was observed in all cases.

DISCUSSION

These studies show that light scattering and turbidity measurements are a quantitative measure of the time dependence and the extent of Mg^{2+}-induced Tm paracrystal formation. The light scattering and sedimentation experiments indicated that the light scattering increment was proportional to the concentration of molecules in the paracrystals. The time course of the light scattering was adequately explained by the helical condensation theory of one-dimensional growth (Oosawa 1962). The data at pH 7.5 was reasonably fit to such a scheme involving

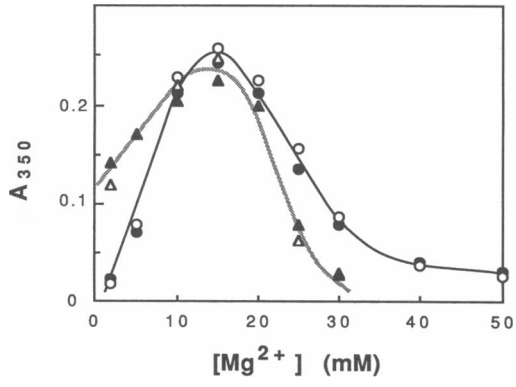

FIGURE 9 Mg^{2+} dependence of paracrystal formation of Tm in the presence of troponin. (○,●), pH 7.5 (20 mM Hepes) or (△,▲) pH 6.0 (20 mM Mes). Experiment was done by adding $MgCl_2$ to Tm-troponin complex in 0.05 mM $CaCl_2$ (*filled symbols*) or 1 mM EGTA (*open symbols*). Turbidity was measured after 2 h incubation. [Tm] = 1.23 μM and [Tn] = 1.23 μM. 25°C.

nucleation and elongation processes and gave values for the nucleus size, i, and an overall rate constant. Slight difference between the calculated curves and the data could be explained by taking into account a small amount of fragmentation and/or association of paracrystals. The value $i = 5 \pm 1$ is reasonable considering the structure of the paracrystals (Stewart and McLachlan, 1976). At pH 6.0 the rate of light scattering increase after a long lag was steeper than such a scheme would predict (see data and curve 1 in Fig. 5). The steepness could be explained, however, by considering fragmentation of the paracrystals, which increases the apparent rate of paracrystal formation by increasing the number of available ends (Oosawa and Asakura, 1975; Wegner and Savko, 1982). The fragmentation appears more probable at pH 6.0 than at pH 7.5 in view of the different paracrystal structures. At pH 6.0 at high Mg^{2+} concentrations it is probable that the fragmentation is suppressed resulting in slow rate of paracrystal formation and large increase in turbidity.

Mg^{2+}-induced Tm paracrystal formation is affected by salt, temperature, and pH. NaCl was found to destabilize the paracrystals by increasing the critical concentration and decreasing the overall rate constants. NaCl appears to act by shielding favorable electrostatic interactions because Na^+ does not bind competitively to the Mg^{2+} binding sites (Oosawa, 1971). Mg^{2+} operates in two opposing ways. At low Mg^{2+} concentration, where Mg^{2+} binding to Tm appears to be low, only a fraction of Tm would form paracrystals and an increase in the critical concentration and a slow rate of paracrystal formation would be expected (Frieden, 1985; Oosawa and Asakura, 1975). $MgCl_2$ concentrations above 15 mM appears to destabilize paracrystals by affecting the critical concentration and overall rate constant in a similar way to NaCl, i.e., by a general ionic strength effect. As a result of the two effects an optimum Mg^{2+} concentration for paracrystal formation is produced which was found to be 15 mM at pH 7.5. This value is not affected by salt, temperature, and even the presence of troponin. A similar value has been reported for the formation of paracrystals in an other coiled-coil system, myosin subfragment-2 (Ueno et al., 1983). Greater concentrations of Tm (5–10 mg/ml) and Mg^{2+} concentrations (~50 mM) are conventionally used to make Tm paracrystals at Tris-HCl buffer (pH 8) (Cohen and Longley, 1966; Caspar, Cohen and Longley, 1969). Under such conditions it is possible that the optimum Mg^{2+} concentration may be higher.

Temperature appears to be important in paracrystal formation affecting both the critical concentration and the rate of paracrystal formation. At low temperature the light scattering gradually increased with Tm concentration around the critical concentration, i.e., the concentration of the dispersed Tm gradually reached the critical concentration. Similar effects were observed at low Mg^{2+}

concentration. This indicates that free-energy required for the formation of nuclei is small compared with that required for elongation (Oosawa and Asakura, 1975).

Paracrystal formation at pH = 6.0 differs from pH 7.5 although the basic condensation process is similar. Evidence for different paracrystal structures was obtained by a study of the pyrene excimer fluorescence of labeled Tm associated with paracrystal formation. This indicated that the Cys-190 regions of adjacent molecules interact for the pH 7.5 paracrystal's but do not for the pH 6 paracrystals. This agrees with structure studies that showed different paracrystal structures formed at the two pH values. At pH > 7, anti-parallel molecular layers, with a 150 A stagger, juxtaposes Cys-190's of adjacent molecules (McLachlan and Stewart, 1975); at pH 6 a smaller stagger (50 A) results in a long distance between Cys of adjacent Tm molecules. The small stagger in the pH 6 paracrystals that keeps overlapping ends closer together may make it easier for fragmentation to take place, a process suggested above to contribute to the different kinetics at pH 6.0. The greater overlapping at pH 7.5 would inhibit fragmentation (brick wall effect). The difference in the paracrystal structure could be explained by the protonation of carboxylate groups protonated between pH 7 and 6 (Cowgill, 1968; Iida and Imai, 1969).

Differences found in paracrystal formation at pH 6.0 compared with pH 7.5 include; (*a*) Tm can form paracrystals over wider range of Mg^{2+} concentration as low as 2 mM and as high as 35 mM in our experimental conditions, (*b*) the critical concentration is almost zero in the absence of NaCl, (*c*) the critical concentration is less salt-dependent, and (*d*) the apparent rate (condensation processes and/or fragmentation) is more temperature-dependent. These observations could be explained by the reduction in negative charge at pH 6.0, which would be expected to decrease electrostatic effects, decrease Mg^{2+} binding and crosslinking by Mg^{2+} and thereby increase the relative contribution of hydrophobic vs. electrostatic interactions. The early finding that Tm forms paracrystals with a small spacing (60–70 A) even in the absence of Mg^{2+} at lower pH (5.4) (Caspar et al., 1969) is consistent with the further reduction in negative charge as the isoelectric point at pH 4.5 is approached.

The presence of troponin does not change the characteristic features of the paracrystal formation of Tm at pH 7.5 but does at pH 6.0. This qualitatively agrees with the observation of different paracrystal structures in the presence of troponin (Nonomura et al., 1968). At pH 7.5 Tm-troponin paracrystals has the same periodicity of 400 A as Tm paracrystals but at pH 6.0 its periodicity is 380 A, a little shorter than that at pH 7.5 and definitely different from Tm paracrystals at pH 6.0 (50 and 70 A) (Nonomura et al., 1968). Thus different profiles of Tm paracrystal formation seem to correlate with its different structure in the presence and absence of troponin.

We would like to thank Professor Fumio Oosawa for valuable suggestions and discussions, and Dr. John Gergely for reading the manuscript.

This work was supported by grants from National Institutes of Health HL-22461 and the National Science Foundation PCM-8213053.

Received for publication 24 October 1988 and in final form 23 February 1989.

REFERENCES

Caspar, D. L. D, C. Cohen, and W. Longley. 1969. Tropomyosin:crystal structure, polymorphism, and molecular interactions. *J. Mol. Biol.* 41:81–107.

Cohen, C., and W. Longley. 1966. Tropomyosin paracrystals formed by divalent cation. *Science. (Wash. DC.).* 152:794–796.

Cowgill, R. W. 1968. Fluorescence and protein structure XIV. Tyrosine fluorescence in helical muscle proteins. *Biochim. Biophys. Acta.* 168:417–430.

Ebashi, S., and M. Endo. 1968. Calcium ion and muscle contraction. *Prog. Biophys. Mol. Biol.* 18:123–183.

Frieden, C. 1985. Actin and tubulin polymerization: the use of kinetic methods to determine mechanism. *Annu. Rev. Biophys. Biophys. Chem.* 14:189–210.

Graceffa, P., and S. S. Lehrer. 1980. The excimer fluorescence of pyrene-labeled tropomyosin. *J. Biol. Chem.* 225:11296–11300.

Iida, S., and N. Imai. 1969. Hydrogen ion titration and sodium ion activity of tropomyosin solutions. *J. Phys. Chem.* 73:75–80.

Katayama, E., and Y. Nonomura. 1979. Electron microscopic analysis of tropomyosin paracrystals. *J. Biochem. (Tokyo).* 86:1511–1522.

Leavis, P., and J. Gergely. 1984. Thin filament proteins and thin filament-linked regulation of vertebrate muscle contraction. *CRC Crit. Rev. Biochem* 16:235–305.

Lehrer, S. S., and Y. Ishii. 1988. Fluorescence properties of acrylodan-labeled tropomyosin and tropomyosin-actin; evidence for myosin subfragment 1 induced changes in geometry between tropomyosin and actin. *Biochemistry.* 27:5899–5906.

Lehrer, S. S., and E. P. Morris. 1982. Dual effects of tropomyosin and troponin-tropomyosin on actomyosin subfragment 1 ATPase. *J. Biol. Chem.* 251:8073–8080.

Longley, W. 1977. A new crystalline form of tropomyosin. *J. Mol. Biol.* 115:381–387.

McLachlan, A. D., and M. Stewart. 1975. Tropomyosin coiled-coil interaction; evidence for an unstaggered structure. *J. Mol. Biol.* 98:293–304.

Nonomura, Y., W. Drabikowski, and S. Ebashi. 1968. The localization of troponin in tropomyosin paracrystals. *J. Biochem. (Tokyo).* 64:419–422.

Ooi, T., K. Mihashi, and H. Kobayashi. 1962. On the polymerization of tropomyosin. *Arch. Biochem. Biophys.* 98:1–11.

Oosawa, F. 1962. Theory of linear and helical aggregation of macromolecules. *J. Mol. Biol.* 4:10–21.

Oosawa, F. 1971. Polyelectrolytes. Marcel Dekker, Inc. New York.

Oosawa, F., and S. Asakura. 1975. Thermodynamics of the polymerization of protein. Academic Press Inc., London.

Smillie, L. B. 1979. Structure and function of tropomyosins from muscle and non-muscle sources. *Trends Biochem. Sci.* 4:151–155.

Stewart, M., and M. D. McLachlan. 1976. Structure of magnesium pracrystals of tropomyosin. *J. Mol. Biol.* 103:251–269.

Ueno, H., M. E. Rodgers, and W. F. Harrington. 1983. Self-association of a high molecular weight subfragment-2 of myosin induced by divalent metal ions. *J Mol. Biol.* 168:207–228.

Wegner, A., and J. Engel. 1975. Kinetics of the cooperative association of actin to actin filament. *Biophys. Chem.* 3:215–225.

Wegner, A., and P. Savko. 1982. Fragmentation of actin filaments. *Biochemistry.* 21:1909–1913.